Localization of the Subendocardial Injury from 12-lead ECG with Moving Equivalent Dipole of the ST Segment

Vito Starc[1], Cees A Swenne[2], Anton P.M. Gorgels[3]

[1]University of Ljubljana, Faculty of Medicine, Ljubljana, Slovenia
[2]Cardiology Department, Leiden University Medical Center, Leiden, the Netherlands
[3]School for Cardiovascular Diseases, Maastricht University, Maastricht, the Netherlands

Abstract

Subendocardial injury (SI) on the 12-lead ECG reflects reduced subendocardial blood flow, but standard ST/T criteria for the anteroseptal (INJAS) and anterolateral (INJAL) regions do not reliably localize the ischemic myocardium. We tested whether the moving equivalent dipole (MED), reconstructed from the 12-lead ECG using a boundary-element torso model, can improve this localization.

MEDs were determined during the ST segment in PTB-XL recordings with annotated INJAS/INJAL (learning set) and in STAFF III patients undergoing elective balloon coronary occlusion, comparing MED behavior during baseline SI and occlusion ischemia. MED vectors were projected onto a 12-segment ventricular model to obtain ventricular surface points (VSPs).

SI-related VSPs clustered mainly in the anteroseptal-basal and inferior segments, mostly pointing toward the base rather than the apex. During occlusion, VSPs shifted toward segments consistent with the occluded vessel and largely reverted after restitution.

An enhanced MED model with non-dipole factors reproduced measured potentials with RNMSE 3.7–4.5%, preserving 95.5–96.3% of ECG information. MED-based vectorcardiography can provide spatial information beyond ST-segment analysis to characterize SI.

1. Introduction

Subendocardial injury (SI) on an electrocardiogram (ECG) is a type of ECG finding that is supposed to indicate a possible lack of blood flow and oxygen to the heart muscle in the subendocardial layer [1]. Injury currents in subendocardial ischemia, presenting as NSTE-ACS, produce ST-segment depressions and T-wave inversions on the 12-lead ECG. SI related to the anterolateral region (INJAL) includes ECG leads V3-V6, I, and aVL, whereas that related to the anteroseptal region (INJAS) includes leads V1-V4. However, these changes do not reliably indicate the ischemic region.

The differential diagnosis is much broader and includes partial occlusion of a coronary artery, as well as any other stress on the body that could cause a supply-and-demand mismatch between the oxygen the coronary arteries can deliver and the oxygen the heart needs.

This study investigates whether modeling cardiac electrical activity using the moving equivalent dipole (MED) approach during the ST segment and T wave can improve ischemia localization. Here, MED is represented by the instantaneous dipole vector, with dipole strength and direction, and its spatial location [2].

Recently, we studied acute myocardial ischemia by determining moving equivalent dipoles (MED) from 12-lead ECG. We have shown that in acute myocardial ischemia due to coronary artery occlusion, the MED orients and moves toward the affected myocardial region [3]. We wondered whether determining MEDs during SI could also provide information about the localization of the process.

2. Methods

2.1. The patients and study protocol

Ischemic ECG recordings were obtained from the PTBXL and STAFF III databases. The PTB XL database provided the annotated INJAL and INJAS ECGs, 36 and 118, respectively [4,5]. This database was used as a learning set to determine MEDs during the ST segment and at the peak of the T wave, thereby allocating the affected myocardial region.

The STAFF III database included 103 patients who underwent elective balloon angioplasty for coronary artery occlusions (RCA, LCX, or LDA), with the vessel occluded for up to 5 minutes [6]. We selected 27 of them in which the concomitant baselines before and after the occlusion also exhibited ECG signs of INJAL or INJAS. In those patients, we compared MED-related data during occlusion ischemia with apparent SI at baseline.

We were particularly interested in whether the

occlusion led to similar or different ECG changes and MED responses, and whether the responses were concordant or discordant. Finally, we were interested in whether the therapeutic procedure had resolved SI, as evidenced by baseline recovery a day after artery occlusion.

Ischemic ECG recordings were obtained from 103 patients within the STAFF III database who underwent elective coronary artery occlusion (RCA, LCX, and LDA). In 42 of them, the concomitant baselines before and after the occlusion also exhibited ECG signs of SI. In those patients, we compared MED-related data during occlusion ischemia and during SI.

2.2. Determination of MEDs - the BEM method

To determine MEDs from the 12-lead ECG, we solved the inverse problem utilizing our boundary element model (BEM) method with an adaptable human torso model [2]. The BEM provides the equation, $\mathbf{V_{ikj}} = \mathbf{L_i(r_k)}\cdot\mathbf{p_j}$, relating the MED properties (dipole vector $\mathbf{p_j}$, and its location $\mathbf{r_{k,j}}$ at time instant j) to the surface potentials Vikj at the lead location $\mathbf{r_i}$. Here $\mathbf{L_{ik}}$ represents the lead vector field (original equation $\boldsymbol{\varphi} = \mathbf{A^{-1}.g}$ in [7]). In inverse solving, the dipole vector $\mathbf{p`_j}$ can be estimated from any given location $\mathbf{r_k}$ and the measured potential $\mathbf{V_{ik}}$ when solved in least-squares terms: Vik = $\mathbf{p`_j}$. In the forward solving that follows, the $\mathbf{p`_j}$ estimate enables the provision of the instantaneous model-predicted electrode potentials, $\mathbf{p`_j} \rightarrow \mathbf{U_{ik}}$. The optimization is achieved by varying rk for each j to minimize the error between the predicted and measured potentials, $\mathbf{U}_{ij}$ and $\mathbf{V}_{ij}$, respectively, with the objective function ψ:

$$\psi = \mathrm{RNMSE} + \sum_i^{N_i}\left(\sum_j^{N_j}\|R\|\right), \text{ where}$$

$$RNMSE = \sqrt{\sum_i^9\sum_j^N\left(\boldsymbol{U_{ij}}-V_{ij}\right)^2}\Big/\sqrt{\sum_i^9\sum_j^N V_{ij}^2} \quad (1)$$

The term R consists of positive-valued regularization functions associated with the optimization parameters [8].

2.3. The optimization strategy

The optimization strategy involves a stepwise trajectory assessment achieved by: 1) dividing the PQRST interval into progressively smaller segments, incorporating an increasing number of optimization parameters; 2) each successive step initiates with MED locations from the previous step. To assess dipolar properties and locations throughout the cardiac, we varied MEDs to minimize the difference between the measured and calculated potentials.

2.4. Construction of a tailored torso model

The torso framework consisted of 24 vertically aligned, rounded isosceles trapezoids with circles inscribed at each trapezoid's corners. Dividing each trapezoid into 48 sectors yielded 1152 discretized surfaces for the outer torso. The torso shape could be modified using the tailor's measures, such as height, waist width, and depth. We created five torsos of different shapes and equal volume by combining torso measures (tall–short, wide-narrow, and thin–thick) that differed by 15%.

2.5. ECG signal processing

All recordings were five-minute (or longer) supine resting 12-lead ECGs (sampling rate of 1 kHz, 300 Hz low-pass filter) providing nine signals (VR, VL, VF, V1…V6) necessary to assess MEDs. After identifying beats, we constructed a template signal by averaging the five most similar beats and delineated the ECG waves.

2.6. The heart model to represent MEDs

We constructed an appropriately oriented bi-ellipsoidal heart model using cardiac MRI data, including the left (LV) and right (RV) ventricles. The heart's long axis coincided with the LV axis, whereas the short axis, perpendicular to the former, pointed at the septum center.

Due to the uncertainty of realistic reference location in the absence of imaging data, we attached the reference location to the heart's mass center point obtained from cardiac MRI studies [9], assuming that the ED trajectory center coincides with the center of the bi-ventricular heart. This procedure helped visualize MEDs in the heart's local coordinate system, enabling description along the short and long axes and in the four-chamber views (Figure 1).

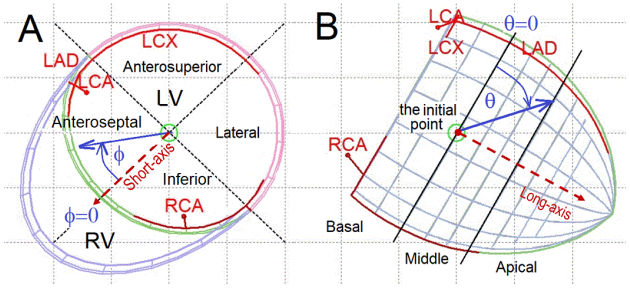

Figure 1. A: The short axis view with the wall segments. B: The long axis view with the wall regions. RCA, LCA, LAD, and LCX are the coronary arteries.

We used a 12-segment LV subdivision with four quadrants (1: anteroseptal, 2: anterosuperior, 3: lateral, 4: inferior), enumerated by Roman numerals in Figure 2A, and three regions (1: apical, 2: middle, 3: basal) in Figure 2B [10]. We related quadrants (q) and regions (r) to the

blood-supplying arteries: the left anterior descending (LAD), left circumflex (LCX), and right coronary (RCA) artery. The myocardial segment number (MSN) was provided by

$$MSN = 3q + r. \qquad (2)$$

We considered that LAD supplies segments 1-5 and 10, LCX 6 - 9, and RCA 11-12, respectively. For a more straightforward calculation, we modified the standardized definition of MSN [10], exchanging quadrants 3 and 4 in (2).

The short-axis view defined azimuth as increasing during clockwise rotation, from -180º to 180º. The long-axis view defined elevation as 0 in the equatorial plane and as increasing from the basal to the apical orientation, from -90º to 90º. The azimuthal angle determined the quadrants and the elevation of the regions. Specifically, the quadrants run from 1 to 4 as azimuth increases by 80º, whereas the basal region was defined as -25º, the middle as -25º to 45º, and the apical as 45º.

2.7. Presentation of MED projections onto the ventricular surface

For the purpose of presentation, we constructed an equal-area pseudocylindrical projection of the ellipsoidal ventricular surface, with the horizontal and vertical axes denoting myocardial quadrants and regions, and with MSN in the segment's center (Figure 2). We superimposed the course of the main coronary arteries (LCA, LAD, diagonal, LCX, and RCA) to facilitate reading.

We introduced the ventricular surface point (MED VSP), to which the MED vector points, obtained by intersecting the MED vector with the model ventricular surface. It describes the MED property in terms of the ventricular coordinate system (azimuth, elevation), enabling allocation of the appropriate myocardial segment according to (2).

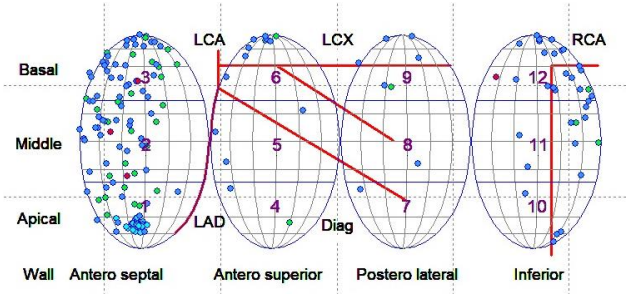

Figure 2. Distribution of the ST segment's MED VSPs of PTBXL ECG recordings with SI. Ventricular segments are annotated by corresponding MSN numbers (1-12). Color coding: INJAS MED VSPs are in blue, INJAL in green, respectively. The apparently healthy population is represented by a cluster at the bottom of Segment 1 in light blue.

3. Results

3.1. Distribution of MED VSPs in the ST segment

The ST segment's MED VSPs in different ischemic states were distributed the following way:

In the apparently normal population VSPs were clustered in ventricular segment 1 (Figure 2, circles in light blue).

In PTBXL with ECG signs of SI, the ST MED VSPs were distributed predominantly in ventricular segments 1, 2, 3, 6, and 12, and much less in segment 11 and rarely in other segments (Figure 2). There was some overlap with the apparently healthy persons in segment 1. In ECGs with INJAL, VSPs were positioned mainly in segments 2 and 3, with some overlap with those in INJAS ECGs.

Interestingly, of 153 cases, 97 (63%) pointed toward the ventricular base, 47 (31%) toward the middle segments, and only 19 (12%) toward the apex.

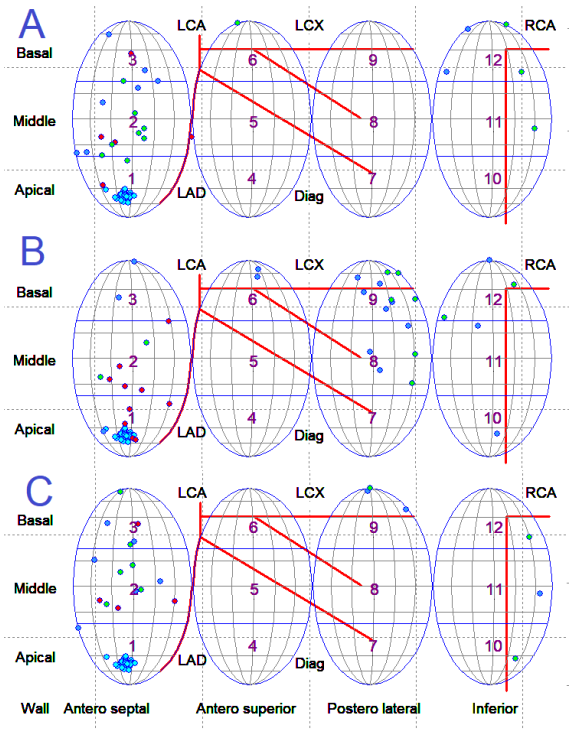

Figure 3. Distribution of the ST segment's MED VSPs of STAFF III baseline ECG recordings with SI. A: Baseline; B: Coronary artery occlusion after 3 minutes; C: Restitution. Color coding considers the occluded vessel: RCA blue, LCX green, and LAD red, respectively. All

other annotations are similar to those of Figure 2.

In the STAFF III database, we identified 27 cases with signs of SI on baseline ECGs. VSPs were distributed similarly to PTBXL in ventricular segments 2, 3, and 12. (Figure 3A). During occlusion, there was a shift of VSPs to segments 1 and 2 in LDA, to 6 and 7 in LCX, and to 1 and 2 in LDA occlusion (Figure 3B). In restitution, VSPs mostly returned to the original ventricular segment.

In patients with baseline SI, the ST segment changed concordantly in 14 cases during occlusion (mostly RCA, less in LCX), and in only two cases was the SI resolved during restitution after the occlusion.

3.2. Quality of the MED assessment

The MED assessment algorithm achieved high consistency between measured and simulated potentials in the 12-lead ECG, with RNMSE values of ~3.7% and ~4.5% for the enhanced model. The results of the three increasingly complex model approaches (FED, MED, and Enhanced MED + non-dipole factors, including the selection of the torso, lead positions, and baseline offset) in Table 1 demonstrate that the dipole orientation used in vectorcardiography accounts for 81 to 85% of the information content. By adding dipole location and non-dipole factors, preserved information increased in the STAFF III database by 4.5% and 6.3%, and in PTBXL by 3.9% and 8.6%, respectively.

Model	STAFF III RNMSE %	PTBXL INJ RNMSE %	STAFF III Preserved information	PTBXL INJ Preserved information
FED	15.0 ± 3.4	18.0 ± 4.0	85.0%	81.1%
MED	7.7 ± 2.0	10.5 ± 3.0	89.5%	89.5%
Enhanced MED	3.7 ± 0.9	4.52 ± 1.2	96.3%	95.5%

4. Discussion and Conclusion

Conclusion: A MED-model-based approach to vectorcardiography, enriched with non-dipole factors, can improve the vectorcardiographic approach of the ECG. The clinical impact of the assessed MED trajectories and vectors deserves further study.

References

[1] N. P. Johnson and K. L.Gould, "Subendocardial ischemia: Does CMD really exist?" Cardiovascular Revasc. Med., vol. 71, p.p. 31–37, 2025.

[2] V. Starc, “Localization of Ischemic Myocardial Segments from 12-Lead ECG Using the Spatial ECG,” *Computing Cardiol.*, vol. 51, pp.1-4, 2023.

[3] V. Starc, and T.T. Schlegel, “Moving dipole determination from 12-lead ECGs can improve detection of acute myocardial Ischemia,” *Computing Cardiol.*, vol. 47, pp.1-4, 2020.

[4] P. Wagner, N. Strodthoff, R. Bousseljot, et al., "PTB-XL, a large publicly available electrocardiography dataset (version 1.0.3)". *PhysioNet*, 2022. RRID:SCR_007345.

[5] Pollard, T., Moody, B. E., Lehman, et al., “PhysioNet as a global platform for biomedical research,“ *Nature Health*, 2026.

[6] S.G. Warren, and G.S. Wagner, "The STAFF studies of the first 5 minutes of percutaneous coronary angioplasty balloon occlusion in man", *J. Electrocardiol.*, vol. 47, pp.402–407, 2014.

[7] T.F. Oostendorp and A. van Oosterom, "Source parameter estimation in inhomogeneous volume conductors of arbitrary shape."*IEEE Trans. Biomed. Eng.*, vol. 36, p.382-391, March 1989.

[8] A.J. Pullan, L.K. Cheng, R. MacLeod, D.H. Brooks, et al., ”The Inverse Problem of Electrocardiography," In PW Macfarlane et al. (eds.), *Comprehensive Electrocardiology*, p. 299-344. Springer, London 2010

[9] F. Odille, S. Liu, P. van Dam, and J. Felblinger, “Statistical. variations of heart orientation in healthy adults,” *Computing Cardiol.*, vol. 44, pp.1-4, 2017.

10] RH Selvester et al., "Myocardial Infarction," In PW Macfarlane et al. (eds), *Comprehensive Electrocardiology*. Springer, London 2010.

[11] M. Potse, A. Vinet, T. Opthof, et al. "Validation of a simple model for the morphology of the T wave in unipolar electrograms," *Am. J. Physiol. Heart. Circ. Physiol.*, vol. 297, pp. H792–H801, 2009.

Address for correspondence:

Vito Starc, MD, PhD
Ljubljana University, Faculty of Medicine
Zaloska 4, SI 1000 Ljubljana, Slovenia
E-mail: vito.starc@mf.uni-lj.si.